Arg-Gly-Asp (RGD) peptide conjugated poly(lactic acid)–poly(ethylene oxide) micelle for targeted drug delivery

Zhiyuan Hu,[1] Fang Luo,[2] Yifeng Pan,[1] Can Hou,[3] Lifeng Ren,[1] Jiji Chen,[1] Jiwei Wang,[1] Yangde Zhang[1]
[1]*Department of Biomedical Engineering, Xiangya Hospital, Central South University, Changsha 410008, China*
[2]*Department of Clinical Medicine, University of South China, Hengyang 421001, China*
[3]*Xiangya Medical College, Central South University, Changsha, Hunan 410008, People's Republic of China*

Received 16 February 2007; revised 15 May 2007; accepted 13 June 2007
Published online 26 September 2007 in Wiley InterScience (www.interscience.wiley.com). DOI: 10.1002/jbm.a.31615

Abstract: In this study, a new poly(lactic acid)–poly (ethylene oxide)-Arg-Gly-Asp (PLA-PEO-RGD) derivative was synthesized, and paclitaxel-loaded PLA-PEO-RGD micelles were prepared by this derivative. The solubility assay showed that micelles mixed with Pluronic F-68 as surfactant could increase the solubility of this hydrophobic paclitaxel in aqueous solution. The cell-binding assay showed that PLA-PEO-RGD micelle (IC_{50} = 11.13 ± 1.38 nmol/L) had about 3.6-fold higher integrin avidity than PLA-PEO-RGD conjugates (IC_{50} = 40.33 ± 3.12 nmol/L). The avidity of micelle was also higher than RGD4C peptide (IC_{50} = 24.44 ± 1.21 nmol/L). The *in vitro* drug release profile of drug-loaded PLA-PEO-RGD micelles exhibited initial burst release to 37% ± 2% (w/w) during the first 12 h, and then the release rate became steady in a controlled release manner. Furthermore, treatment of the MDA-MB-435 breast cancer cell line with paclitaxel-loaded PLA-PEO-RGD micelles yielded cytotoxicities, with EC_{50} values of ~30 μmol/L. The paclitaxel-loaded PLA-PEO-RGD micelles treated group showed the most dramatic tumor reduction in MDA-MB-435 tumor-bearing nude mice, and the final mean tumor load was 31 ± 16 mm^3 (mean ± SD; n = 8). ^{125}I-labeled micelles administration resulted in significant ($p < 0.001$) higher tumor uptake (2.68% ± 0.14%, ID/g) of PLA-PEO-RGD micelles compared to PLA-PEO micelles (0.84% ± 0.09%, ID/g) after 2.5 h postinjection. Biodistribution study showed the best blood clearance of PLA-PEO-RGD micelles after 4.5 h postinjection. The results of this study suggest that paclitaxel-loaded PLA-PEO-RGD micelles based on the specific recognition of $\alpha_V\beta_3$ integrin represent a potential and powerful target delivery technology. © 2007 Wiley Periodicals, Inc. J Biomed Mater Res 85A: 797–807, 2008

Key words: RGD; PLA-PEO; micelle; paclitaxel; $\alpha_V\beta_3$

INTRODUCTION

Currently, a large variety of chemotherapeutic drugs are widely used to treat malignant diseases. Unfortunately, the remarkable antitumor activity exhibited by many cytotoxic drugs is accompanied by undesirable side effects causing severe damage to healthy tissues, and therefore, limiting their efficacy.[1,2] Ligand-mediated chemotherapeutic drug targeting has emerged as a novel paradigm in targeting either vascular compartment (first-order), cellular (second-order), or intracellular (third-order) levels. Most carrier systems or bioconjugates explored so far can be used as cargo units for the site-specific presentation and delivery of various bioactives using biorelevant ligands, including antibodies,[3] polypeptides,[4,5] oligosaccharides (carbohydrates), viral proteins, and fusogenic residues.

A tumor cannot grow beyond the size of 1–2 mm in diameter without developing a blood supply providing oxygen and nutrients. This phenomenon, known as angiogenesis, was hypothesized 30 years ago, by Folkman, to be an absolute requirement for the growth and metastasis of solid tumors.[6,7] Tumor blood vessels exhibit several abnormalities in comparison with normal physiological vessels,[8] which could also constitute potential targets for specific antiangiogenic therapy. Indeed, the vasculature undergoing angiogenesis differs from normal quiescent vasculature by an overexpression of ECM-binding

This article contains supplementary material available via the Internet at http://www.interscience.wiley.com/jpages/1549-3296/suppmat.

Correspondence to: Y. Zhang; e-mail: plapeorgd@yahoo.com.cn or J. Wang; e-mail: jw_wang68@yahoo.com.cn

Contract grant sponsor: National Natural Science Foundation of China; contract grant number: 30400185
Contract grant sponsor: National High Technology Research and Development Project of China; contract grant number: 2002AA216011
Contract grant sponsor: Major State Basic Research Development Program of China; contract grant number: 2004CB518802

integrin receptors such as $\alpha_V\beta_3$ and $\alpha_V\beta_5$. These markers make them suitable targets for chemotherapeutics administration.[9,10] The affinity of Arg-Gly-Asp (RGD) peptides for $\alpha_V\beta_3$ receptors expressed on tumor blood vessels and on some tumoral cells has found major attention. Recently, this property has been exploited to image tumors *in vitro* and *in vivo* using radiolabeled RGD-containing peptides.[11,12] Several researchers also synthesis some RGD conjugates to target tumor angiogenic vasculature.[13,14] RGD-targeted PEG-liposome is a very hopeful candidate in antiangiogenic therapy.[15,16]

In an attempt to provide a selective tumor cells targeting, we chose RGD moieties on poly(lactic acid)-poly(ethylene oxide) (PLA-PEO) colloidal drug-delivery systems. Micellar could be an attractive drug carrier, as it contains many characteristics of ideal drug-delivery systems.[17,18] Micelle can encapsulate various types of drugs, and drugs are protected from possible inactivation by biological surrounding, and also prevent undesirable side effects of cytotoxic drugs.[19] Micellar drug carriers can be made to specifically target certain cells by designing specific ligands on the outer surface of micelles. DNA and RNA sequences, oligosaccharides, peptides, and specific antibodies can serve as ligands used in drug targeting. There are several examples of targeted biopharmaceuticals conjugates such as antibody conjugates, enzyme–antibody conjugates, and folate-bearing conjugates, and cell adhesion molecule targeting conjugates.[20]

PLA-PEO diblock polymer contains hydrophobic PLA chain and hydrophilic PEO chain. PLA has been extensively investigated for applications in drug delivery.[21] It is biodegradable, well adapted to biological environments, and does not have adverse effects on blood and tissues. PEO has the advantage of being hydrophilic, nonionic, and biocompatible, and it has also been used in various biomedical applications for increasing the stability of blood contacting materials.[22,23] Due to such unique properties, broad interest on copolymers of PEO/PLA with AB and ABA architecture has been generated for the use in biomedical applications.[24–28]

In this study, a novel PLA-PEG-RGD conjugate has been prepared; the conjugate has many characteristics to be an ideal drug carrier. This conjugate can enclose drug molecule inside the core of micelle to protect drug from degradation as well as prevent unwanted drug interactions. And also the shell of the micelle containing RGD binding moiety will exhibit enhanced binding, due to several integrins overexpressed on many types of cancer cells to help deliver the drug molecule to a specific site of action. Also, we selected a lipophilic anticancer drug paclitaxel as model drug to assess the efficacy of these bioconjugates *in vitro* and *in vivo* using a MDA-MB-435 tumor-bearing nude mouse model. We now report an example of micellar bioconjugates that exhibit significant anticancer efficacy without the systemic toxicity that is common to chemotherapeutics.

MATERIALS AND METHODS

Materials

Bicyclic RGD4C (ACDCRGDCFCG, molecular weight [M_w] 1145.3) was obtained from AnaSpec. 4,4′-Methylene di-phenyl diisocyanate (MDI, CAS number: 101-68-8, $C_{15}H_{10}N_2O_2$) and poly(ethylene glycol) (PEG, M_w = 1450) were purchased from Sigma-Aldrich. Poly(D,L-lactic acid) (PLA, M_w = 15,000) was purchased from Shandong Medical Instrument Institute (Qingdao, China). Toluene, diethyl ether, methylene chloride, and acetone were purchased from SinoPharm (Beijing, China). Di-*n*-butyltin dilaurate was purchased from Stable Chemical (Beijing, China). Methyl sulfonyl chloride (chemical reagent) was used without further purification. Triethylamine was purified according to the commonly used method.[29]

Cell lines

MDA-MB-435 breast carcinoma cells were purchased from Experimental Center of Central South University of China. Cells were cultured in RPMI medium 1640 (Sigma) supplemented with 10% FBS (Min Hai Bio, Qinghai, China). Cells were grown at 37°C in a humidified atmosphere of 5% CO_2 (v/v) in air. All experiments were performed on cells in the exponential growth phase.

Preparation of paclitaxel-loaded PLA-PEO-RGD (or PLA-PEO) nanomicelle

The methods of PLA-PEO diblock polymer and PLA-PEO RGD derivative preparation are in supporting files. The paclitaxel-loaded PLA-PEO-RGD nanomicelle was prepared using an oil-in-water emulsion–solvent evaporation method, conveniently adapted to obtain nanomicelle. Briefly, 1.25 mg paclitaxel and 2.5 mg PLA-PEO-RGD (or 2.5 mg PLA-PEO) conjugates were dissolved in 5 mL of dichloromethane. The organic solution was added into a volume of 20 mL of a 0.5% (w/v) Pluronic F-68 aqueous solution and the two phases were emulsified for 1.5 min with a high speed homogenizer (ULTRA-TURRAX T-25 Basic, IKA, Germany). The organic solvent was then eliminated by evaporation under 50°C. Finally, the particles were isolated from centrifugation (3k18; Sigma, Germany; 15,000 rpm, 30 min) and washed three times with water.

Solubility degree assay

An excess amount of paclitaxel was added into deionized water and was shaken at 100 rpm for 24 h at 24°C. The undissolved paclitaxel was filtered. Paclitaxel-loaded

PLA-PEO-RGD micelle solution was prepared in the upper step. Another paclitaxel-loaded PLA-PEO-RGD micelle solution was prepared with the same method but without surfactant Pluronic F-68 in aqueous solution. These three samples were then lyophilized (Labconco®, Kansas) for 48 h to obtain dry powder. Powder was redissolved in ethanol. The concentration of paclitaxel in these three samples was determined by the method of HPLC. The mobile phase used for high performance liquid chromatography (HPLC) analysis of paclitaxel was a mixture of methanol/ethanol/water (30:40:30) at a flow rate of 1 mL/min. A C18 reverse phase column was used, and paclitaxel was detected spectrophotometrically at 235 nm. The HPLC system used consisted of a Waters 590 HPLC pump (Waters, Milford, MA), Hitachi L-7200 auto-sampler (Hitachi, Tokyo, Japan).

Receptor-binding assay

Binding affinity of the PLA-PEO-RGD micelles to $\alpha_v\beta_3$ integrin on the surface of MDA-MB-435 cells was determined in competitive binding experiments using ^{125}I-labeled echistatin as radioligand as described in the literature with modifications.[30] In brief, MDA-MB-435 cells were grown in Dulbecco's medium (Gibco) supplemented with 10% fetal bovine serum (FBS), 100 IU/mL penicillin, and 100 μg/mL streptomycin (Invitrogen), at 37°C in a humidified atmosphere containing 5% CO_2. During the cell-binding assay experiment, the cells were harvested, washed twice with PBS, and resuspended (2×10^6 cells/mL) in binding buffer (20 mmol/L Tris, pH 7.4, 150 mmol/L NaCl, 2 mmol/L $CaCl_2$, 1 mmol/L $MgCl_2$, 1 mmol/L $MnCl_2$, 0.1% bovine serum albumin). Filter multiscreen DV plates (96-well; pore size, 0.65 μm; Millipore) were seeded with 10^5 cells and incubated with ^{125}I-echistatin (30,000 cpm/well) in the presence of increasing concentrations of different RGD peptide analogs (PLA-PEO-RGD micelle, RGD4C and PLA-PEO-RGD conjugate) (0–1000 nmol/L). The total incubation volume was adjusted to 200 μL. After the cells were incubated for 3 h at room temperature, the plate was filtered through multiscreen vacuum manifold and washed twice with cold binding buffer. The hydrophilic PVDF filters were collected, and the radioactivity was determined using NaI (Tl) γ-counter (Packard, Meriden, CT). The best-fit IC_{50} values for the MDA-MB-435 cells were calculated by fitting the data by nonlinear regression using Origin (OriginLab Corporation, Northampton, MA). Experiments were carried out with triplicate samples.

In vitro release of paclitaxel

Two milligrams of lyophilized drug-loaded nanoparticles were redispersed in 10 mL of phosphate buffer solution (PBS, pH 7.4 containing 0.1%, w/v, Tween 80) in a capped centrifuge tube. The tube was placed in a shaking incubator (120 cycles/min) at 37°C. Tween 80 was used to increase the solubility of paclitaxel in the release medium and to reduce the association of the drug with the container surface. At predetermined times, the tube was centrifuged at 39,000*g* for 20 min. The collected particles were redispersed in 10 mL fresh PBS, containing Tween 80, for continuous release studies. The release of paclitaxel in the supernatant was extracted with 2 mL DCM and then 1 mL of acetonitrile/water (50/50, v/v) was added to the extract. After DCM was evaporated by a dry nitrogen stream, the drug concentration in the clear solution was analyzed by HPLC. The HPLC apparatus was equipped with a Waters 510 solvent delivery pump, a Luna C18(2) column (5 μm, 250 mm × 4.6 mm; Phenomenex, USA), and a UV/vis detector (Laballiance, USA), operated at a wavelength of 227 nm. The mobile phase was acetonitrile/water (50/50, v/v) and the flow rate was 1.0 mL/min. The concentration of drug in the solution was obtained from the calibration curve.

In vitro cytotoxicity assay

The cytotoxicity of paclitaxel-loaded micelles against MDA-MB-435 cells was measured by MTT assay. MDA-MB-435 cells of passages between 20 and 24 were cultured in DMEM supplemented with 10% heat-inactivated FBS, 100 units/mL penicillin, 100 μg/mL streptomycin, and 0.25 μg/mL amphotericin B, under 5% CO_2 at 37°C. The cells were inoculated to a 96-well plate at a density of 10^4 cells in 200 μL medium per well, and incubated for 24 h. Medium was replenished every 2 days. The medium was then replaced with PLA-PEO-RGD micelles-containing media (empty loaded micelles and paclitaxel-loaded micelles with the drug concentration ranging from 0 to 100 μmol/mL) and incubation was continued as earlier for 24 h. The micelles-containing media were removed, and 180 μL fresh medium and 20 μL MTT solution (5 mg/mL in PBS) were added to the cells. The cells were incubated for 3 h. MTT internalization was terminated by aspiration of the media, and the cells were lysed with DMSO. The optical density at 570 nm was determined using a microplate reader (Genios, Tecan, Männedorf, Switzerland).

Xenograft tumor model

All animal experiments were performed with the approval from Institutional Animal Care and Use Committee. One week before MDA-MB-435 cells inoculation, each mice received 2 μg of 17β-oestradiol valerate (Sigma), dissolved in 0.2 mL of sesame oil, by subcutaneous injection. Oestrogen injections were repeated every week to sustain tumor growth. Nude mice were inoculated subcutaneously with 2×10^7 MDA-MB-435 cells. By day 35 after inoculation, all of the tumors were about the same size (≈300 mm^3). The animals were randomly distributed into five groups at eight mice each. Using the previously reported maximal tolerated dose (MTD) of 20 mg/kg for i.v. paclitaxel[19] as a reference point, the following regimens were administered by tail vein injections once a week: (1) saline; (2) PLA-PEO-RGD nanomicelle without drug; (3) paclitaxel-loaded PLA-PEO nanomicelle (PPP), 20 mg/kg paclitaxel; (4) paclitaxel, 20 mg/kg; or (5) paclitaxel-loaded PLA-PEO-RGD nanomicelle (PPP-RGD), 20 mg/kg paclitaxel. The tumor size and body weight were then monitored for

7 weeks. Tumor growth was measured twice a week using a caliper (in mm) and tumor weight (mg) was calculated using the formula tumor weight (mg) = $(a^2 \times b)/2$, where a is the width in mm and b is the length in mm. Micelles used *in vivo* were all prepared using Pluronic F-68 as surfactant.

Apoptosis

The approach to assess apoptosis induction was based on the measurement of the enrichment of histone-associated DNA fragments (mono- and oligonucleosomes) in homogenates of the tumor and different organs (liver, kidney, spleen, heart, and lung) by using anti-histone and anti-DNA antibodies by a cell death detection ELISA^{PLUS} kit (Roche Applied Biosciences) as described.[31,32] Briefly, the isolated cells of organs and tumor were harvested after treatment, and incubated on ice for 30 min in Tris lysis buffer (50 m*M* Tris-HCl, pH 7.5, 150 m*M* NaCl, 1 m*M* EDTA, 20 m*M* NaF, 0.5% NP-40, and 1% Triton X-100) containing fresh protease inhibitors (5 μg/mL aprotinin, 10 μg/mL phenylmethylsulfonyl fluoride, and 10 μg/mL sodium vanadate), and then centrifuged at 14,000*g* for 10 min at 4°C. The total cell lysate was used for protein determination by the DC Bio-Rad® protein assay. The lysate was added to lysis buffer and pipetted on a streptavidin-coated 96-well microtiter plate to which immunoreagent mix was added and incubated for 2 h at room temperature with continuous shaking at 600*g*. The wells were then washed with washing buffer, the substrate solution added, and the color developed (10–20 min) was read at 405 nm against the blank, reference wavelength of 490 nm. In these experiments, there were only three tumors that could be analyzed in PPP-RGD treatment group, since five of eight treated animals experienced complete tumor reductions.

Organ distribution of PLA-PEO and PLA-PEO-RGD micelle

Copolymers PLA-PEO and PLA-PEO-RGD were radiolabeled with ^{125}I in the 1,4-dioxane medium by a modified chloramine T method.[33] Each of the copolymers (30 mg) was dissolved in 1 mL of 1,4-dioxane. Then 10 mL of [^{125}I] iodide (100 μL/mL) (ICN Biomedicals, Irvine, CA) was added. The reaction was started by addition of 40 mL of a chloramine T solution (50 mg/mL) in phosphate buffer (pH 7.4). The solution was tightly capped, and the reaction was allowed to proceed with stirring for 24 h. The reaction was stopped by addition of 60 mL of sodium metabisulfite solution (100 mg/mL). Unbound [^{125}I] iodide was displaced by addition of 20 mL of potassium iodide (100 mg/mL). Unbound ^{125}I was removed by dialysis. Then the radiolabeled copolymer was used for preparing nanomicelle by the method described in "Materials and Methods" with Pluronic F-68 as surfactant. But these micelles used for the biodistribution study did not carry paclitaxel. All biodistribution studies of tumor and organ (liver, kidney, spleen, heart, lung, and brain) were obtained under the same experimental conditions. When the tumors reached a size of ≈300 mm^3, mice were treated i.v. with 15 mg/kg ^{125}I-labeled PLA-PEO-RGD nanomicelle and ^{125}I-labeled PLA-PEO nanomicelle. The maximum tolerated dose was detected in separate experiments. The animals were euthanized at 0.5, 1.5, 2.5, and 4.5 h postinjection. Tissues were removed and the radioactivity uptakes, expressed in %ID/g were measured. The activity of ^{125}I in samples of tumor and tissues was measured with gamma counter Wallac 1480 Wizard 3 (Wallac, Turku, Finland). Student's two-tailed unpaired t-test was performed to determine statistical significance of the observed differences in organ accumulation between the conjugates.

RESULTS

Micelle preparation

In the emulsification step of preparation process, the hydrophilic RGD peptide fixed to PEO blocks migrated to the water interface, whereas the PLA blocks and paclitaxel remained within the organic droplets. After organic solvent dichloromethane removal, micelles with paclitaxel central core and a grafted PEO-RGD hydrophilic shell were formed. The surface morphology and size distribution of nanomicelles were evaluated by transmission electron microscope (TEM) (Fig. 1). The mean particle size was 128 ± 10 nm. This image was typical of those obtained for all the samples, confirming that the PLA-PEO-RGD bioconjugates form spherical, discrete particles in aqueous media.

Enhancement of solubility of paclitaxel encapsulated in micelle

The solubility of paclitaxel in water was used as a reference for comparison with solubility enhancement of other samples. The solubility for paclitaxel in water was determined to be 0.23 μg/mL (Table I). The solubility of paclitaxel encapsulated in PLA-PEO-RGD micelle prepared by the method without surfactant Pluronic F-68 was determined to be 0.40 μg/mL

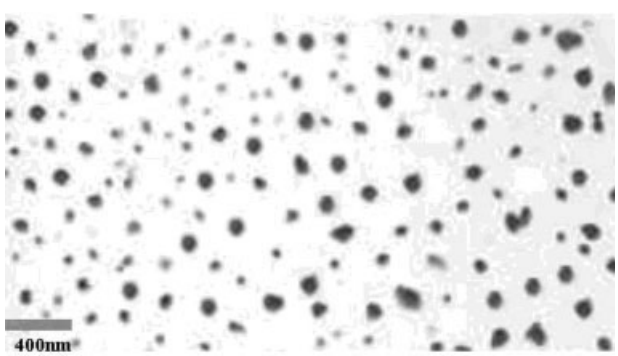

Figure 1. TEM photograph of PLA-PEO-RGD micelle.

TABLE I
Study of Solubility of Paclitaxel

Sample, $n = 3$	Solubility ± SD (μg/mL)	Solubility Enhancement (%)
Paclitaxel in water, no surfactant	0.23 ± 0.02	Baseline
Pa in micelle no surfactant[a]	0.40 ± 0.04	73.9
Pa in micelle with surfactant[b]	1.42 ± 0.25	617

[a]Pa in micelle no surfactant: Paclitaxel encapsulated in PLA-PEO-RGD micelle without surfactant.
[b]Pa in micelle with surfactant: Paclitaxel in encapsulated in PLA-PEO-RGD micelle with surfactant Pluronic F-68.

(Table I). PLA-PEO-RGD micelle prepared without surfactant enhanced the solubility of the paclitaxel by 73.9%. The solubility of paclitaxel (1.42 μg/mL) in PLA-PEO-RGD micelle solution prepared by adding Pluronic F-68 as surfactant showed this surfactant can increase the solubility of paclitaxel by 6.17 fold (Table I). These solubility enhancement results showed that PLA-PEO-RGD micelle with surfactant can increase the solubility of hydrophobic paclitaxel.

Integrin binding affinity

To compare the binding affinity of PLA-PEO-RGD micelle with other RGD peptide conjugates, competitive binding measurements were performed between ^{125}I-echistatin and the RGD analogs (PLA-PEO-RGD conjugate and RGD4C peptide) (Fig. 2). All analogs tested in these assays showed the expected sigmoid curves. They inhibited the binding of ^{125}I-echistatin to α_v integrin-positive MDA-MB-435 cells. The IC_{50} values for echistatin, PLA-PEO-RGD micelle, RGD peptide, and PLA-PEO-RGD conjugate were 0.25 ± 0.01, 11.13 ± 1.38, 24.44 ± 1.21, and 40.33 ± 3.12 nmol/L, respectively. The cell-binding assay demonstrated that PLA-PEO-RGD micelle had about 3.6-fold higher integrin avidity than PLA-PEO-RGD conjugate. The avidity of micelle was also higher than RGD4C peptide. Coupling of PLA-PEO chain with RGD4C peptide significantly reduce the receptor avidity of the peptide (IC_{50} values for RGD4C peptide and PLA-PEO-RGD conjugate were 24.44 ± 1.21 and 40.33 ± 3.12 nmol/L, respectively). But once PLA-PEO-RGD conjugate was used for preparing micelle by using an oil-in-water emulsion–solvent evaporation method; the receptor avidity of RGD was significantly upgraded. The reason may be that amphiphilic PLA-PEO-RGD block copolymers form micelles composed of a hydrophobic PLA core and hydrophilic RGD shell in water. Hydrophobic blocks are segregated from the aqueous exterior to form an inner core surrounded by a palisade of hydrophilic segments. Micelles with nanometer-scale size have large ratio of surface to bulk atoms. Large surface always gives high active behavior of RGD. The nanometer-scale property of micelles enhanced the receptor avidity of RGD in our experiments.

In vivo release profile

The amount of paclitaxel released from drug-loaded micelles was determined in an *in vitro* release assay, in an effort to assess whether paclitaxel-incorporating micelles might be useful as a sustained-release dosage form. Drug-loaded micelles were incubated in PBS at 37°C. The *in vitro* release profiles of paclitaxel from paclitaxel-loaded PLA-PEO-RGD micelles into PBS (pH 7.4) solution are presented in Figure 3. Paclitaxel-loaded micelles exhibit an initial burst release to 37% ± 2% (w/w) during the first 12 h, and then the release rate of paclitaxel slowed down and became steady in a controlled-release manner.

In vitro cytotoxicity

To assess the cytotoxicity of paclitaxel-loaded PLA-PEO-RGD micelles, their tumor cell killing activity was determined against breast cancer cell lines by MTT assay. Paclitaxel-free PLA-PEO-RGD micelles did not cause significant cytotoxicity against MDA-MB-435 cells up to the concentration 10 μmol/L

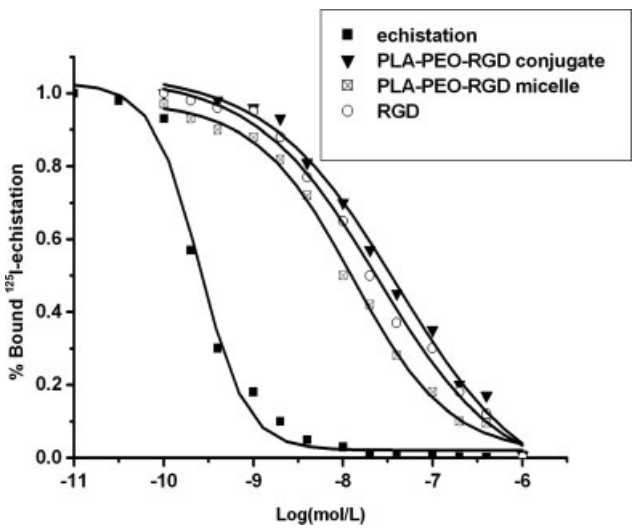

Figure 2. Competition of specific binding of ^{125}I-echistatin with unlabeled echistatin (■), RGD4C (○), PLA-PEO-RGD micelle (⊠), and PLA-PEO-RGD conjugate (▼) to MDA-MB-435 cells. Cell-associated radioactivity in the absence of competitor was set at 100%. Values are mean of triplicate assays ± SD. [echistatin: 0.25 ± 0.01 nmol/L; PLA-PEO-RGD micelle: 11.13 ± 1.38 nmol/L; RGD peptide: 24.44 ± 1.21 nmol/L; PLA-PEO-RGD conjugate: 40.33 ± 3.12 nmol/L].

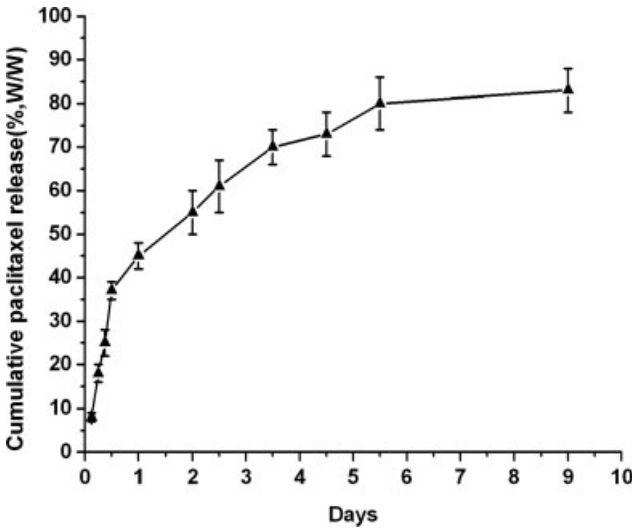

Figure 3. *In vitro* cumulative paclitaxel release (mean ± SD, $n = 3$) profile for paclitaxel-loaded PLA-PEO-RGD micelles prepared by emulsion methods.

(survival = 90% ± 5% for concentration 10 μmol/L). However, the empty micelles did show cytotoxicity at higher dose (survival = 82% ± 8% for concentration 100 μmol/L) (Fig. 4). Paclitaxel-loaded micelles showed cytotoxicity against MDA-MB-435 cells, with EC_{50} values of ~30 μmol/L.

In vivo effect of tumor growth inhibiting

For saline, PLA-PEO-RGD, and paclitaxel groups, the treatment did not show good efficacy at the end of observation period, and the mean tumor sizes at the end of the study for the groups were 1223 ± 39, 1220 ± 56, and 398 ± 15 mm^3, respectively (mean ± SD; $n = 8$) [Fig. 5(a)]. None of the animals of the saline and PLA-PEO-RGD groups exhibited tumor regression. Overall five of seven animals in the saline group and six of eight animals in the PLA-PEO-RGD group reached end point (body weight loss of >20%) during the study duration. Five of the eight animals in the paclitaxel group reached the end point [Fig. 5(b)]. The difference in the final mean tumor size for the paclitaxel group compared with the saline and PLA-PEO-RGD groups was statistically significant. The paclitaxel-PLA-PEO-RGD-treated group demonstrated the most dramatic efficacy: the final mean tumor load was 31 ± 16 mm^3 (mean ± SD, $n = 8$, significantly smaller than all other groups by ANOVA at 95% confidence interval). Five of eight treated animals experienced complete tumor reductions. Another animal exhibited regression of tumor size after the initial dosing, remaining animals showed tumor growth after treatment. Only three tumors could be analyzed, since five mice were completely free of tumor at the end of the treatment. All mice in the paclitaxel-PLA-PEO-RGD group survived the 6 weeks study duration. The paclitaxel-PLA-PEO group also was more efficacious than the paclitaxel, PAL-PEO-RGD, and saline control groups, but significantly less efficacious when compared with the paclitaxel-PLA-PEO-RGD group. The mean tumor size at end point was 145 ± 15 mm^3 (mean ± SD, $n = 8$). Two complete tumor reductions were observed and three animals dead during study duration. The study demonstrated that, after a single administration, the paclitaxel-loaded PLA-PEO-RGD micelle group was most efficacious against MDA-MB-435 cells breast tumors, resulting in a better survival than other treatment groups.

Apoptosis induction

The analysis of apoptosis induction in the tumor and the healthy organs confirmed the effectiveness of the tumor-targeting approach in comparison with the paclitaxel alone and paclitaxel-PLA-PEO (Fig. 4). The direct measurement of apoptosis induction in the tumor and the healthy organs showed that passive targeting because of the enhanced permeability and retention effect led to a decrease in the induction of apoptosis in healthy organs and enhanced the apoptosis induction in the tumor. However, "active" tumor targeting by RGD peptide dramatically increased apoptosis induction in the tumor and significantly prevented adverse events on healthy tissues; apoptosis induction level in the tumor by paclitaxel-PLA-PEO-RGD group is 51 ± 7 (Fig. 6). We can see that paclitaxel alone use has adverse events on healthy tissues;

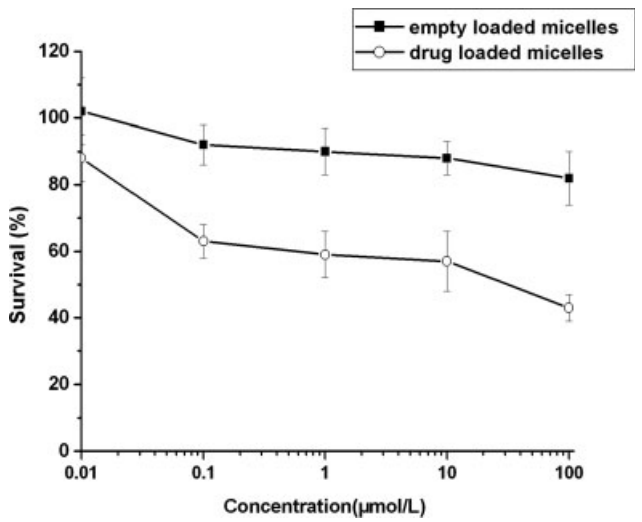

Figure 4. Dose-dependent cytotoxicity of paclitaxel-loaded micelles against MDA-MB-435 cells. Cells were treated with empty (solid square) and paclitaxel-loaded micelles (empty circle). The utilized concentration of empty micelles was that at which the micelles could deliver the designated paclitaxel concentration. Each point represents the mean ± SD from three experiments.

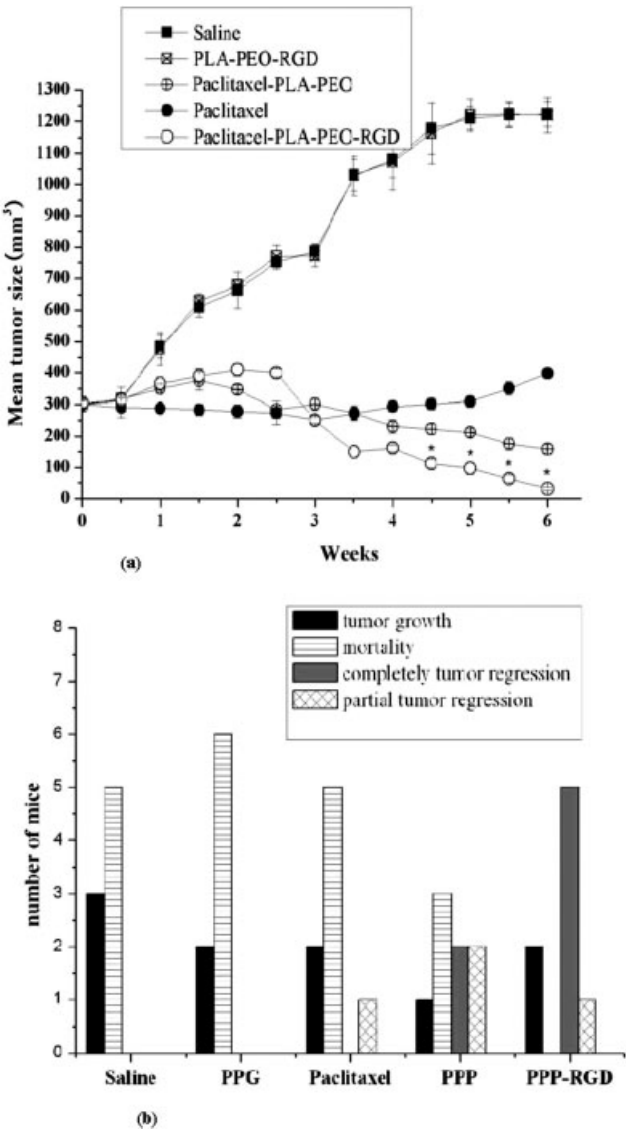

Figure 5. (a) The comparative efficacy study of single tail vein injection (day 0) of (i) saline (solid square); (ii) PLA-PEO-RGD(PP-RGD) nanomicelle without drug (× center square); (iii) paclitaxel loaded PLA-PEO(PPP) nanomicelle (+ center circle), 40 mg/kg; (iv) paclitaxel (solid circle), 40 mg/kg; or (v) paclitaxel-loaded PLA-PEO-RGD(PPP-RGD) nanomicelle (circle), 40 mg/kg paclitaxel. (b) Plot of results for each of the five groups divided into four categories: tumor growth (black), complete tumor regression (gray), partial tumor regression (grid), and mortality (bar). There were only three tumors that could be analyzed in PPP-RGD treatment group, since five of eight treated animals experienced complete tumor reductions.

the apoptosis level of paclitaxel to liver, spleen, kidney, heart, and lung are 7.9 ± 0.4, 7.3 ± 0.8, 7.2 ± 0.5, 8.3 ± 0.4, and 7.8 ± 0.6, respectively (Fig. 6).

Biodistribution

To verify that the PLA-PEO-RGD conjugates could specifically target human breast cancer xenografts

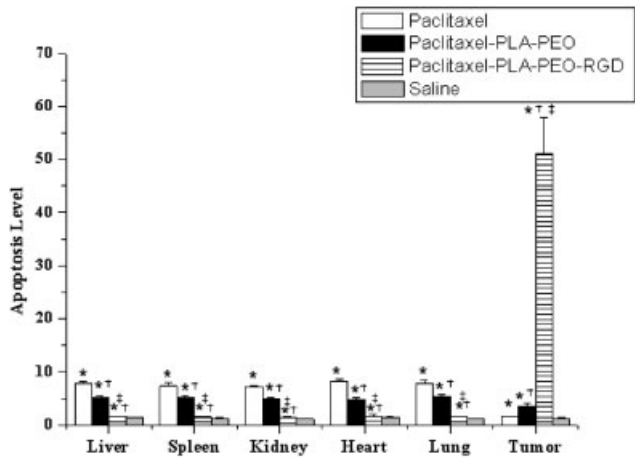

Figure 6. Apoptosis induced by treating with saline (control), paclitaxel, paclitaxel-PLA-PEO, and paclitaxel-PLA-PEO-RGD in tumor and different tissues in mice bearing xenograft of breast tumor. *, $p < 0.05$ when compared with mice treated with saline; †, $p < 0.05$ when compared with mice treated with paclitaxel; ‡, $p < 0.05$ when compared with mice treated with paclitaxel-PLA-PEO.

in vivo, the biodistributions of ^{125}I-labeled PLA-PEO-RGD micelles and ^{125}I-labeled PLA-PEO micelles in mice were evaluated. Tumor accumulation was significantly ($p < 0.001$) higher for the PLA-PEO-RGD micelles [3.53% ± 0.14% ID/g; tumor (T)/blood (B) = 17.65] than for the PLA-PEO micelles [0.84% ± 0.09% ID/g; T/B = 3.36]. Kidney and liver accumulation were also observed for the PLA-PEO-RGD micelles (5.1% ± 0.3%, 2.3% ± 0.2%, respectively), and the PLA-PEO micelle (7.4% ± 0.2%, 6.5% ± 0.1%, respectively) (Fig. 7).

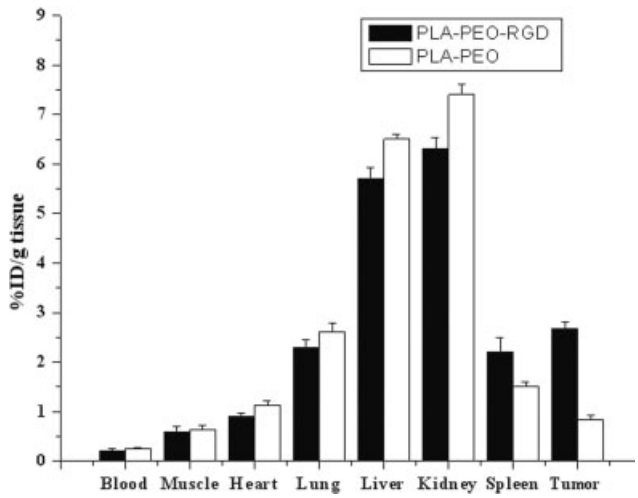

Figure 7. The radioactivity in tissues and tumor 2.5 h postintravenous injection of ^{125}I-labeled residual radioactivity in percent injected dose per gram (% ID/g) of organ tissue 2.5 h postintravenous injection of ^{125}I-labeled conjugates. The tumor localization of PLA-PEO-RGD nanomicelle (black) is significantly ($p < 0.001$) greater than PLA-PEO nanomicelle (white). The data are expressed as mean ± SD.

A different time-points biodistribution study was carried out to better assess the extended *in vivo* accumulation and clearance of PLA-PEO-RGD micelle. The results seen in Figure 8 demonstrate a time-dependent decrease of PLA-PEO-RGD micelle accumulation in all organs analyzed except the tumor. PLA-PEO-RGD micelle revealed fast blood and organ clearance. The accumulation of blood, liver, kidney, heart, and muscle at 4.5 h was significantly ($p < 0.05$) lower than at 0.5 h, respectively. The lung accumulation at 4.5 h was significantly ($p < 0.05$) lower than at 2.5 h. The maximum tumor uptake for the micelle appeared at 2.5 h postinjection (3.53% ± 0.14% ID/g), and remained constant at 4.5 h postinjection (3.30% ± 0.13% ID/g). The best tumor-to-blood and tumor-to-organ ratios were achieved at 4.5 h postinjection. The maximum tumor/blood ratio at 4.5 h (33.00) was significantly ($p < 0.05$) higher than the ratio at 2.5 h (17.65); also the ratio at 2.5 h was significantly ($p < 0.05$) higher than at 0.5 h (1.75). The tumor/blood ratios increase significantly over time indicating rapid blood clearance and sustained tumor accumulation (Fig. 9).

The discovery of RGD sequence, the cell attachment site of many other adhesive proteins,[34,35] and the subsequent discovery of integrins, cell surface receptors that recognize the RGD sequence of various proteins, have given RGD a central role in cell adhesion biology as the prototype adhesion signal. The rapid advancement of the understanding of the function of RGD has impacted the design and development of drugs with the potential to treat cancer by inhibiting tumor angiogenesis.

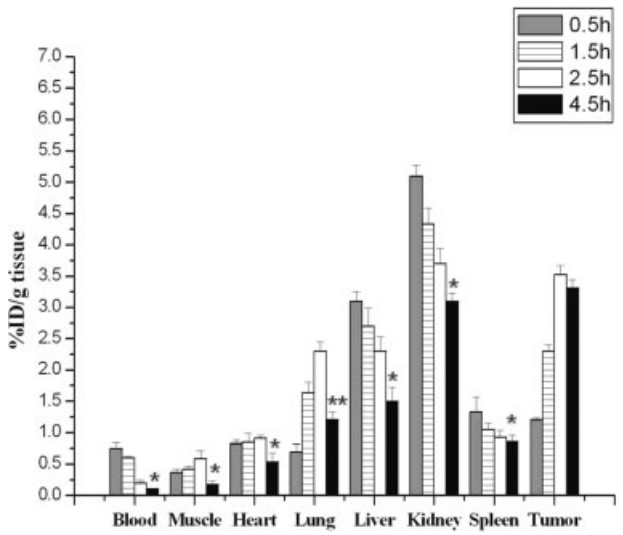

Figure 8. Different time-points radioactivity, expressed as percent injected dose per gram tissue (% ID/g) in different organs and tumor of MDA-MB-435 xenograft model after intravenous injection of ^{125}I-labeled PLA-PEO-RGD nanomicelle at 0.5, 1.5, 2.5, and 4.5 h ($n = 4$). *$p < 0.05$ compared to 0.5 h, **$p < 0.05$ compared to 2.5 h.

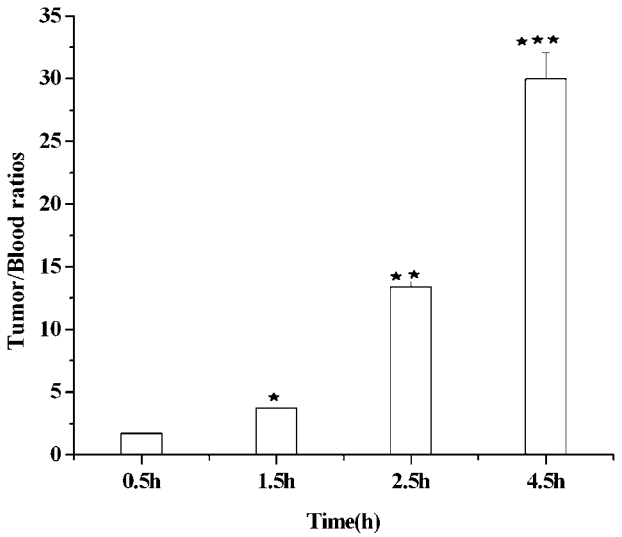

Figure 9. Tumor/blood ratios of PLA-PEO-RGD 0.5, 1.5, 2.5, and 4.5 h postintravenous injection. The ratios increment has significant time dependence demonstrating rapid blood clearance and sustained tumor accumulation. The data are expressed as mean ± SD ($n = 4$). *$p < 0.05$ compared to 0.5 h, **$p < 0.05$ compared to 0.5 and 1.5 h, ***$p < 0.05$ compared to 0.5, 1.5, and 2.5 h.

Micelles 10–100 nm in size can deliver large payloads to molecular targets, but undergo slow diffusion and/or slow transport through delivery barriers.[36] So we used the binding of RGD peptide PLA-PEO micelle targeting integrins on MDA-MB-435 tumor-bearing nude mice. Integrin-targeting micelles showed a better blood clearance and rapid tumor accumulation (Fig. 8). This targeting strategy presents a very hopeful target delivery method. Amphiphilic molecules (PLA-PEO-RGD) could spontaneously organize into micelles and displayed the targeting motif on the micellar surface, which was recognized by the integrin receptors on breast cancer cells surface and internalized by cells via receptor mediated endocytosis to deliver paclitaxel. These micelles contained an inner core that could encapsulate and increase the solubility of hydrophobic paclitaxel, which could potentially mask the toxicity of paclitaxel until delivery to specifically targeted cells.

DISCUSSION

Specific *in vivo* tumor targeting was demonstrated by the 3.19-fold higher tumor localization with PLA-PEO-RGD micelles relative to PLA-PEO micelles after 2.5 h postinjection. The best tumor/blood ratio for PLA-PEO-RGD micelles was also achieved after 4.5 h postinjection. The higher tumor accumulation was due to the high affinity of RGD peptides to $\alpha_V\beta_3$ integrin. The PLA-PEO micelles showed a

lower tumor uptake relative to PLA-PEO-RGD micelles, as these micelles accumulate in tumor through a mechanism called the Enhanced Permeability and Retention (EPR) effect. This EPR effect can be attributed to these micelles that had long blood circulation to escape the vasculature through abnormal leaky tumor blood vessels.[37]

As pluronic F-68 has only very low toxicity,[38] Pluronic F-68 nonionic surfactant has diverse applications in various biomedical fields ranging from controlling release of drugs and also as a coating for wounds and protection against microbes.[39–41] Subsequent to the approval by the U.S. Food and Drug Administration, this substance has been found to have widespread use in the medical field as vehicle for delivery of drugs through the rectal, ophthalmic, and nasal mucosa, as well as for subcutaneous administration.[39-41] The available toxicology LD_{50} data[42] for poloxamers are based on oral and dermal dosing, which is less than 5 g/kg body weight. The kinetics and fate of radiolabeled pluronic F-68 following intravenous administration has been determined in dogs.[43] Radiolabeled pluronic F-68 has been found in all organs, particularly in the liver, lung, and muscles, 24 h postintravenous administration into the dog. This study has indicated that the primary route of pluronic F-68 excretion is renal, and that the minor route is biliary.[43]

To target $\alpha_V\beta_3$-integrin expressing tumor vasculature, RGD peptides have been conjugated to liposomes,[15,16] polymer[44,45] by chemical methods. *In vivo* long-term biodistribution evaluation in tumor-bearing mice was carried out in Amitava Mitra's research. The tumor accumulation increased significantly ($p < 0.01$) over time from 1.05% ± 0.03% ID/g tissue at 1 h to 4.32% ± 0.32% at 72 h. In contrast, the activity in major background tissues (blood, liver, spleen, and kidney) decreased significantly ($p < 0.05$) from 1 to 72 h postinjection in SCID mouse xenograft model of human prostate carcinoma.[45] In our studies, the maximum tumor uptake for the PLA-PEO-RGD nanomicelle appeared at 2.5 h postinjection (3.53% ± 0.14% ID/g), and remained constant at 4.5 h postinjection (3.30% ± 0.13% ID/g). Xenograft model of human breast cancer of our study showed faster tumor accumulation of conjugate than xenograft model of human prostate carcinoma in Amitava Mitra's research. The antitumor effectiveness of HPMA copolymer-RGD4C conjugate in a SCID mouse xenograft model of human prostate carcinoma was also evaluated in Amitava Mitra's research. At 21 days, the control tumors increased 442% in volume from baseline. In contrast, a 7% and a 63% decrease of tumor volume were observed for the 100- and 250-μCi ^{90}Y-labeled HPMA copolymer-RGD4C conjugates treatment groups, respectively.[45] In our experiments, after 6 weeks observation time, the control tumors increased 307.7% in volume from baseline. In contrast, an 89.7% decrease of tumor volume was observed for the paclitaxel-loaded PLA-PEO-RGD micelle treatment group.

The distribution levels of PLA-PEO-RGD micelle in the liver, spleen, and kidney are comparable to the tumor uptake. But the apoptosis experiment data did not show an increase in apoptosis level in these organs (Fig. 6). In Bruce R. Line and Amitava Mitra's studies of HPMA copolymer-RGD4C conjugates biodistribution, although the organ activity for the polymer–peptide conjugates was lower than the free peptide, the levels in the liver, spleen, and kidney are comparable to or higher than the tumor uptake.[44] After paclitaxel-loaded copolymer–peptide micelles were accumulated in kidney, liver, and spleen, copolymer–peptide micelle did not interact with the cell easily as there was less $\alpha_V\beta_3$ integrin in these organs than tumor. Also paclitaxel did not leak in these organs temporarily, as paclitaxel was encapsulated in micelle core with RGD peptide outside of micelle. Then micelles showed organ elimination and tumor accumulation as longer blood circulation times were observed for copolymer–peptide micelles. The increased tumor intensity for the micelles was most likely due to the interaction of the $\alpha_V\beta_3$ integrin with the RGD motifs on the micelle surface. The $\alpha_V\beta_3$ target was immediately accessible to the intravascular space of tumor. Increased apoptosis levels were not observed in the liver, spleen, and kidney due to the long blood circulation, paclitaxel encapsulation in core, and specific $\alpha_V\beta_3$ integrin targeting of micelle.

Xiaoyuan Chen' research showed that the IC_{50} values for echistatin, $E\{E[c(RGDfK)]_2\}_2$, and $E[c(RGDfK)]_2$ to human glioblastoma U87MG cell line were 1.2 ± 0.1, 15.0 ± 1.1, and 32.2 ± 2.1 nmol/L, respectively. The IC_{50} values for DOTA-$E\{E[c(RGDfK)]_2\}_2$ and DOTA-$E[c(RGDfK)]_2$ were 16.6 ± 1.3 and 48.4 ± 2.8 nmol/L.[30] In our integrin binding affinity assay, the IC_{50} values for echistatin, PLA-PEO-RGD micelle, RGD4C peptide, and PLA-PEO-RGD conjugate to MDA-MB-435 cells were 0.25 ± 0.01, 11.13 ± 1.38, 24.44 ± 1.21, and 40.33 ± 3.12 nmol/L, respectively. Integrin avidity of PLA-PEO-RGD micelle to MDA-MB-435 cells was higher than DOTA-$E\{E[c(RGDfK)]_2\}_2$ to human glioblastoma U87MG cells. The affinity of RGD4C was higher than $E[c(RGDfK)]_2$, but lower than $E\{E[c(RGDfK)]_2\}_2$. The endothelial cell adhesion assay results of Amitava Mitra's research[46] also indicated that free RGD4C showed 1.3-fold higher inhibition than free RGDfK.

CONCLUSIONS

In our study, a diblock copolymer was successfully synthesized by a coupling reaction between

poly(D,L-lactic acid) and PEG through MDI. RGD were then attached to the end of PEO chain. Then we developed controlled-release polymer drug-delivery vehicles, which could target and be taken up by MDA-MB-435 cells. The solubility assay of paclitaxel showed that the enhancement of paclitaxel solubility could be achieved by encapsulating this hydrophobic drug in PLA-PEO-RGD micelle, and the surfactant used in micelle preparation could increase the solubility by 6.17 fold. PLA-PEO-RGD micelle was shown to bind with high affinity and specificity with integrin-positive MDA-MB-435 cells *in vitro*.

The release behavior of paclitaxel from drug-loaded micelles exhibited a biphasic pattern characterized by a fast initial release, followed by a slower and continuous release. *In vitro* cell viability experiment for MDA-MB-435 cells showed high cytotoxicity of paclitaxel in the micelle formulation, with EC_{50} values of $\sim$30 μmol/L. *In vivo* effect of tumor growth inhibiting showed that paclitaxel-loaded PLA-PEO-RGD micelles were more efficacious against MDA-MB-435 cells xenograft tumor than paclitaxel and paclitaxel-loaded PLA-PEO micelles. Biodistribution study showed that PLA-PEO-RGD micelles had specific localization in tumor and decreased accumulation in all organs analyzed except the tumor and rapid blood clearance.

References

1. Duncan R. Polymer conjugates for tumour targeting and intracytoplasmic delivery. The EPR effect as a common gateway? Pharm Sci Technol Today 1999;2:441–449.
2. Torchilin VP. Drug targeting. Eur J Pharm Sci 2000;11(Suppl 2):S81–S91.
3. Marty C, Schwendener RA. Cytotoxic tumor targeting with scFv antibody-modified liposomes. Methods Mol Med 2005; 109:389–402.
4. Wickham TJ. Ligand-directed targeting of genes to the site of disease. Nat Med 2003;9:135–139.
5. Shi G, Guo W, Stephenson SM, Lee RJ. Efficient intracellular drug and gene delivery using folate receptor-targeted pH-sensitive liposomes composed of cationic/anionic lipid combinations. J Control Release 2002;80:309–319.
6. Naumov GN, Akslen LA, Folkman J. Role of angiogenesis in human tumor dormancy: Animal models of the angiogenic switch. Cell Cycle 2006;5:1779–1787.
7. Folkman J. Tumor angiogenesis: Therapeutic implications. N Engl J Med 1971;285:1182–1186.
8. Ruoslahti E, Rajotte D. An address system in the vasculature of normal tissues and tumors. Annu Rev Immunol 2000;18: 813–827.
9. Sheu JR, Yen MH, Kan YC, Hung WC, Chang PT, Luk HN. Inhibition of angiogenesis in vitro and in vivo: Comparison of the relative activities of triflavin, an Arg-Gly-Asp-containing peptide and anti-α(v)β3 integrin monoclonal antibody. Biochim Biophys Acta 1997;1336:445–454.
10. Meyer T, Hart IR. Mechanisms of tumour metastasis. Eur J Cancer 1998;34:214–221.
11. Benjamin LE, Golijanin D, Itin A, Pode D, Keshet E. Selective ablation of immature blood vessels in established human tumors follows vascular endothelial growth factor withdrawal. J Clin Invest 1999;103:159–165.
12. Haubner R, Wester HJ, Burkhart F, Senekowitsch-Schmidtke R, Weber W, Goodman SL, Kessler H, Schwaiger M. Glycosylated RGD-containing peptides: Tracer for tumor targeting and angiogenesis imaging with improved biokinetics. J Nucl Med 2001;42:326–336.
13. Bibby DC, Talmadge JE, Dalal MK, Kurz SG, Chytil KM, Barry SE, Shand DG, Steiert M. Pharmacokinetics and biodistribution of RGD-targeted doxorubicin-loaded nanoparticles in tumor-bearing mice. Int J Pharm 2005;293:281–290.
14. Jasseron S, Contino-Pepin C, Maurizis JC, Rapp M, Pucci B. Synthesis and preliminary biological assessments of RGD bearing biocompatible telomers. Bioorg Med Chem Lett 2002; 12:1067–1070.
15. Janssen AP, Schiffelers RM, ten Hagen TL, Koning GA, Schraa AJ, Kok RJ, Storm G, Molema G. Peptide-targeted PEG-liposomes in anti-angiogenic therapy. Int J Pharm 2003;254:55–58.
16. Schiffelers RM, Koning GA, ten Hagen TL, Fens MH, Schraa AJ, Janssen AP, Kok RJ, Molema G, Storm G. Anti-tumor efficacy of tumor vasculature-targeted liposomal doxorubicin. J Control Release 2003;91:115–122.
17. Jones M, Leroux J. Polymeric micelles—A new generation of colloidal drug carriers. Eur J Pharm Biopharm 1999;48:101–111.
18. Nakayama M, Okano T, Miyazaki T, Kohori F, Sakai K, Yokoyama M. Molecular design of biodegradable polymeric micelles for temperature-responsive drug release. J Control Release 2006;115:46–56.
19. Kim SC, Kim DW, Shim YH, Bang JS, Oh HS, Kim SW, Seo MH. In vivo evaluation of polymeric micellar paclitaxel formulation: Toxicity and efficacy. J Control Release 2001;72: 191–202.
20. Willis M, Forssen E. Ligand-targeted liposomes. Adv Drug Deliv Rev 1998;29:249–271.
21. Simamora P, Chern W. Poly-L-lactic acid: An overview. J Drugs Dermatol 2006;5:436–440.
22. Gref R, Minamitake Y, Peracchia MT, Trubetskoy V, Torchilin V, Langer R. Biodegradable long-circulating polymeric nanospheres. Science 1994;263:1600–1603.
23. Langer R. New methods of drug delivery. Science 1990;249: 1527–1533.
24. Kissel T, Li Y, Unger F. ABA-triblock copolymers from biodegradable polyester A-blocks and hydrophilic poly(ethylene oxide) B-blocks as a candidate for in situ forming hydrogel delivery systems for proteins. Adv Drug Deliv Rev 2002;54: 99–134.
25. Molina I, Li S, Martinez MB, Vert M. Protein release from physically crosslinked hydrogels of the PLA/PEO/PLA triblock copolymer-type. Biomaterials 2001;22:363–369.
26. Li S, Molina I, Martinez MB, Vert M. Hydrolytic and enzymatic degradations of physically crosslinked hydrogels prepared from PLA/PEO/PLA triblock copolymers. J Mater Sci Mater Med 2002;13:81–86.
27. Agrawal SK, Sanabria-DeLong N, Coburn JM, Tew GN, Bhatia SR. Novel drug release profiles from micellar solutions of PLA-PEO-PLA triblock copolymers. J Control Release 2006; 112:64–71.
28. De Jaeghere F, Allemann E, Leroux JC, Stevels W, Feijen J, Doelker E, Gurny R. Formulation and lyoprotection of poly (lactic acid-*co*-ethylene oxide) nanoparticles: Influence on physical stability and in vitro cell uptake. Pharm Res 1999; 16:859–866.
29. Lemarchand C, Gref R, Passirani C, Garcion E, Petri B, Muller R, Costantini D, Couvreur P. Influence of polysaccharide coating on the interactions of nanoparticles with biological systems. Biomaterials 2006;27:108–118.

30. Wu Y, Zhang X, Xiong Z, Cheng Z, Fisher DR, Liu S, Gambhir SS, Chen X. MicroPET imaging of glioma integrin {alpha}v{beta}3 expression using (64)Cu-labeled tetrameric RGD peptide. J Nucl Med 2005;46:1707–1718.
31. Minko T, Kopeckova P, Kopecek J. Efficacy of the chemotherapeutic action of HPMA copolymer-bound doxorubicin in a solid tumor model of ovarian carcinoma. Int J Cancer 2000;86:108–117.
32. Pakunlu RI, Wang Y, Tsao W, Pozharov V, Cook TJ, Minko T. Enhancement of the efficacy of chemotherapy for lung cancer by simultaneous suppression of multidrug resistance and antiapoptotic cellular defense: Novel multicomponent delivery system. Cancer Res 2004;64:6214–6224.
33. Bridges JF, Critchlow M, Irving MP, Purkiss SC, Taylor DC, Lloyd JB. Radiolabeling, stability, and body distribution in rats, of low molecular weight polylactide homopolymer and polylactide-polyethyleneglycol copolymer. Biomaterials 2000; 21:199–209.
34. Pierschbacher MD, Ruoslahti E. Variants of the cell recognition site of fibronectin that retain attachment-promoting activity. Proc Natl Acad Sci USA 1984;81:5985–5988.
35. Yamada KM, Kennedy DW. Dualistic nature of adhesive protein function: Fibronectin and its biologically active peptide fragments can autoinhibit fibronectin function. J Cell Biol 1984;99(1, Part 1):29–36.
36. Montet X, Montet-Abou K, Reynolds F, Weissleder R, Josephson L. Nanoparticle imaging of integrins on tumor cells. Neoplasia 2006;8:214–222.
37. Koziara JM, Whisman TR, Tseng MT, Mumper RJ. In-vivo efficacy of novel paclitaxel nanoparticles in paclitaxel-resistant human colorectal tumors. J Control Release 2006;112:312–319.
38. Magnusson G, Olsson T, Nyberg JA. Toxicity of Pluronic F-68. Toxicol Lett 1986;30:203–207.
39. Petri B, Bootz A, Khalansky A, Hekmatara T, Muller R, Uhl R, Kreuter J, Gelperina S. Chemotherapy of brain tumour using doxorubicin bound to surfactant-coated poly(butyl cyanoacrylate) nanoparticles: Revisiting the role of surfactants. J Control Release 2007;117:51–58.
40. Pisal SS, Paradkar AR, Mahadik KR, Kadam SS. Pluronic gels for nasal delivery of Vitamin B12, Part 1: Preformulation study. Int J Pharm 2004;270:37–45.
41. Marsh LH, Alexander C, Coke M, Dettmar PW, Havler M, Nevell TG, Smart JD, Timmins B, Tsibouklis J. Adsorbed pluronics on the skin of human volunteers: Effects on bacterial adhesion. Int J Pharm 2003;251:155–163.
42. BASF Corporation. BASF Performance Chemicals Catalogue. New Jersey: Pluronic® & Tetronic® Surfactants BASF Corporation; 1996. 70 p.
43. Willcox ML, Newman MM, Paton BC. A study of labeled pluronic F-68 after intravenous injection into the dog. J Surg Res 1978;25:349–356.
44. Line BR, Mitra A, Nan A, Ghandehari H. Targeting tumor angiogenesis: Comparison of peptide and polymer–peptide conjugates. J Nucl Med 2005;46:1552–1560.
45. Mitra A, Nan A, Papadimitriou JC, Ghandehari H, Line BR. Polymer–peptide conjugates for angiogenesis targeted tumor radiotherapy. Nucl Med Biol 2006;33:43–52.
46. Mitra A, Coleman T, Borgman M, Nan A, Ghandehari H, Line BR. Polymeric conjugates of mono- and bi-cyclic αVβ3 binding peptides for tumor targeting. J Control Release 2006; 114:175–183.